REGULAR ARTICLE

blood advances

A single F153Sβ3 mutation causes constitutive integrin αIIbβ3 activation in a variant form of Glanzmann thrombasthenia

Sevasti B. Koukouritaki,[1,2] Aye Myat M. Thinn,[3,4] Katrina J. Ashworth,[5] Juan Fang,[1,2] Haley S. Slater,[1,2] Lily M. Du,[1,2] Huong Thi Thu Nguyen,[3] Xavier Pillois,[6] Alan T. Nurden,[6] Christopher J. Ng,[7] Jorge Di Paola,[5] Jieqing Zhu,[3,4] and David A. Wilcox[1-3]

[1]Department of Pediatrics, Medical College of Wisconsin, Milwaukee, WI; [2]Children's Research Institute, Children's Wisconsin, Milwaukee, WI; [3]Versiti Blood Research Institute, Milwaukee, WI; [4]Department of Biochemistry, Medical College of Wisconsin, Milwaukee, WI; [5]Department of Pediatrics, Division of Hematology & Oncology, Washington University School of Medicine, Washington University in St. Louis, St. Louis, MO; [6]Xavier Arnozan Hôpital, Institut de Rythmologie et de Modélisation Cardiaque, Pessac, France; and [7]Department of Pediatrics, Section of Hematology/Oncology/Bone Marrow Transplant, University of Colorado Anschutz Medical Campus, Aurora, CO

Key Points

- Glanzmann thrombasthenic platelets retain hemostatic function with only low-level expression of a constitutively active mutant form of αIIb-F153Sβ3.
- The bulky aromatic, nonpolar structure of F153β3 amino acid is vital for normal αIIbβ3 integrin shift from resting to an activated state.

This report identifies a novel variant form of the inherited bleeding disorder Glanzmann thrombasthenia, exhibiting only mild bleeding in a physically active individual. The platelets cannot aggregate ex vivo with physiologic agonists of activation, although microfluidic analysis with whole blood displays moderate ex vivo platelet adhesion and aggregation consistent with mild bleeding. Immunocytometry shows reduced expression of αIIbβ3 on quiescent platelets that spontaneously bind/store fibrinogen, and activation-dependent antibodies (ligand-induced binding site–319.4 and PAC-1) report β3 extension suggesting an intrinsic activation phenotype. Genetic analysis reveals a single F153Sβ3 substitution within the βI-domain from a heterozygous T556C nucleotide substitution of *ITGB3* exon 4 in conjunction with a previously reported IVS5(+1)G>A splice site mutation with undetectable platelet messenger RNA accounting for hemizygous expression of S153β3. F153 is completely conserved among β3 of several species and all human β-integrin subunits suggesting that it may play a vital role in integrin structure/function. Mutagenesis of αIIb-F153Sβ3 also displays reduced levels of a constitutively activated αIIb-S153β3 on HEK293T cells. The overall structural analysis suggests that a bulky aromatic, nonpolar amino acid (F,W)153β3 is critical for maintaining the resting conformation of α2- and α1-helices of the βI-domain because small amino acid substitutions (S,A) facilitate an unhindered inward movement of the α2- and α1-helices of the βI-domain toward the constitutively active αIIbβ3 conformation, while a bulky aromatic, polar amino acid (Y) hinders such movements and restrains αIIbβ3 activation. The data collectively demonstrate that disruption of F153β3 can significantly alter normal integrin/platelet function, although reduced expression of αIIb-S153β3 may be compensated by a hyperactive conformation that promotes viable hemostasis.

Submitted 6 December 2022; accepted 27 February 2023; prepublished online on *Blood Advances* First Edition 8 March 2023; final version published online 3 July 2023. https://doi.org/10.1182/bloodadvances.2022009495.

Data are available on request from the corresponding author, David A. Wilcox (dwilcox@mcw.edu).

The full-text version of this article contains a data supplement.

Introduction

Integrin αIIbβ3 is a heterodimer complex present in a quiescent state on the surface of resting platelets, which upon platelet activation assumes an extended conformation that mediates platelet aggregation by binding fibrinogen and other adhesive proteins.[1,2] The receptor also facilitates spreading of platelets on the subendothelial matrix and plays a role in thrombus formation at the site of vascular injury.[3,4] Integrin αIIbβ3 is normally expressed at ~80 000 copies on the platelet surface.[5,6] The genes *ITGA2B* and *ITGB3* encoding αIIb and β3 respectively are colocalized on chromosome 17q21.31-32.[7-9] To date, several hundred unique molecular genetic mutations have been characterized in αIIbβ3 that causes a rare autosomal recessive inherited platelet bleeding disorder named Glanzmann thrombasthenia (GT) after the Swiss pediatrician, Eduard Glanzmann who first described the disorder in 1918.[10,11] The prevalence of GT is estimated to be 1:1 million people.[12] Genetic abnormalities of *ITGA2B* and *ITGB3* cause quantitative and/or qualitative deficiencies of αIIbβ3, which disrupt platelet function leading to uncontrolled bleeding.[13] Platelet function testing is routinely used in combination with immunocytometry that measures the level of αIIb (CD41) and β3 (CD61) on the platelet surface to help provide a clinical diagnosis of GT and distinguish between subtypes I or II.[14] Variant forms of GT have also been reported with moderate to normal levels of a functionally defective αIIbβ3.[15,16] The identification of genetic variations capable of causing GT has accelerated recently through the use of next-generation whole-exome sequence analysis.[17] Genetic defects discovered in *ITGA2B* or *ITGB3* have been organized into an international database managed by the Medical College of Wisconsin (MCW) to assist ongoing efforts to better understand GT. The nature and position of each mutation has helped characterize the relationship between integrin structure and function that plays a vital role in platelet response to vascular injury.[18]

This study explores the significance of a constitutively active form of αIIbβ3 with a novel F153S amino acid (aa) substitution in the βI-domain of β3 expressed at reduced levels on platelets from a patient with a mild form of GT. Functional analysis was performed both on human platelets and transfected cells coexpressing αIIb with different aa forms of 153β3. Our goal is to understand the importance of maintaining the structure of the βI-domain of β3 by establishing the role F153β3 plays in integrin activation. Structural analysis of resting and active β3 conformations highlighted a potential mechanism for the inward movement of the α2-helix that was associated with a well-characterized inward movement of the α1-helix. The results suggest that the 153aa of β3 requires a bulky aromatic and nonpolar side chain under the α2-helix to sterically restrain its unprovoked inward movement toward the active conformation. The bulky to small residue change of F153Sβ3 facilitates an unregulated movement of α2-helix to transform αIIbβ3 into a constitutively active conformation with (1) spontaneous binding of fibrinogen, (2) functional transport of fibrinogen to α-granules, and (3) residual platelet function in a microfluidic assay that may help explain the mild phenotype of the patient.

Material and methods

Patient with GT

A middle-aged Hispanic male diagnosed with GT provided written informed consent to participate in this study approved by the institutional review boards at the Anschutz Medical Campus, University of Colorado (09-0816), Hemo-PICS, and Children's Research Institute of Children's Wisconsin (Milwaukee, WI) (90343-20) Glanzmann Thrombasthenia Human Research. The Versiti Blood Research Institute/Medical College of Wisconsin (PRO00025928) institutional review board approved human blood studies.

Blood collection

Whole blood (2-4 mL) was collected by venipuncture into sodium citrate anticoagulant. Complete blood counts were measured using a Sysmex XP300 (Sysmex America, Lincolnshire, IL) or Hemavet 950 (Drew Scientific, Miami Lakes, FL) (supplemental Table 1). Platelet-rich plasma (PRP) was prepared by centrifugation at 200*g* for 10 minutes. Platelet counts were normalized to $250 \times 10^3/\mu L$. Platelet aggregation and other function tests were performed using standard procedures for platelet activation with thrombin, adenosine diphosphate (ADP), collagen (supplemental Figure 1), or ristocetin (supplemental Table 2) agonists (Ags). Platelets were isolated with Fico/Lite platelets (Atlanta Biologicals, Inc., Lawrenceville, GA), washed with phosphate-buffered saline, and used directly for immunocytometry and immunoblot analysis as previously reported.[19] Aliquots of patient's platelets (1×10^6) were also stored frozen at −80°C until needed.

Microfluidics

Whole blood was assessed for its ability to bind collagen under physiologic shear stress using a microfluidic assay as previously described.[20] Briefly, blood was collected into a vacutube containing sodium heparin. Type I collagen (500 μg/mL) was patterned onto a microfluidic device and platelets in whole blood were labeled with fluorescent dye 3,3′-dihexyloxacarbocyanine iodide (1 μg/mL) and then perfused through the vacuum-sealed microfluidic device at a wall shear rate of 650 s^{-1} for 5 minutes using a PHD 2000 Syringe Pump (Harvard Apparatus, Holliston, MA). Platelet accretion was captured in real time in relief contrast and fluorescence with an Olympus IX81 microscope (Center Valley, PA) using an ORCA Flash4 camera (Hamamatsu, Japan). Images were captured using cellSens software (Center Valley, PA). Platelet surface area covered with time was analyzed using FIJI/ImageJ 1.51n (National Institutes of Health, Bethesda, MD) and data were processed with GraphPad (Dotmatics, Boston, MA).

Immunocytometry

Surface expression of αIIbβ3 on platelets (5×10^6/mL) was analyzed by cytometry using fluorescent-labeled primary monoclonal antibodies (1°mAb) (supplemental Method 1) recognizing human αIIb, β3, and glycoprotein Ibα (GPIbα) as previously described.[19,21] PRP or washed platelets were incubated with 20 μg/mL 1°mAb followed by fluorescein isothiocyanate–conjugated secondary antibody (2°Ab) for 30 minutes. Samples were analyzed with a LSRII or Accuri C6Plus Flow Cytometer (BD Biosciences, San Jose, CA).

Platelet αIIbβ3 integrin activation assays: LIBS exposure, fibrinogen, and PAC-1 binding

Blood samples anticoagulated with sodium citrate were collected to measure integrin activation state as previously described.[22-24] Briefly, PRP or washed platelets were resuspended at 0.2 × 10^8/mL and treated with buffer (—Ag) or agonists of platelet activation (+Ag) consisting of thrombin (ligand-induced binding site [LIBS] Ab), TRAP (fibrinogen molecule), or a TRAP/ADP/epinephrine mixture (P-selectin, PAC-1 Abs) for 30 minutes at room temperature. Platelet and αIIbβ3 activation analysis was detected by measurement of the mean fluorescence intensity (MFI) of binding Alexa-647–labeled goat-anti-mouse immunoglobulin G for 2°Ab (AP3), Alexa-647–labeled Fab 319.4 (LIBS), fluorescein isothiocyanate–PAC-1, phycoerythrin–P-selectin mAbs, or Alexa-488–labeled fibrinogen. Platelet binding was detected by immunocytometry and measurements of MFI in absence (—Ag) or presence of agonist (+Ag) conditions were adjusted to match the total surface β3 levels (AP3) for wild-type (WT) and GT samples, respectively, to normalize the MFI as percentage of β3 receptor density levels. The GRGDW peptide was tested for inhibition of PAC-1 binding αIIbβ3 as previously described.

Electrophoresis and immunoblot quantitation analysis for platelet αIIbβ3 and fibrinogen

Washed platelets were solubilized as described previously.[25] Briefly, protein concentration was determined with a micro bicinchoninic acid protein assay.[26] Solubilized proteins were resolved by sodium dodecyl sulfate polyacrylamide gel electrophoresis and immunoblotted with 1°Ab, and horseradish-conjugated 2°Ab.[27,28] Protein bands were detected by enhanced chemiluminescence according to the manufacturers instructions by exposure on an imager (Amersham, Piscataway, NJ) or Fuji Super RX film (Thermo Fisher Scientific, Pittsburgh, PA) and digitized using a Hewlett Packard 6300C scanner (Boise, ID). The integrated optical density of immunoreactive protein bands were determined using a Kodak DC120 digital camera and Digital Science 1D software (New Haven, CT). Further details are given in supplemental Method 2.

Immunofluorescent confocal microscopy

Human platelets were fixed, permeabilized, blocked, incubated with antifibrinogen 1°Ab and Alexa488-2°Ab and visualized on a confocal microscope as previously described (supplemental Method 3).[29]

Whole blood DNA and platelet mRNA isolation

Genomic DNA (gDNA) was extracted from whole blood using the FlexiGene DNA Kit (Qiagen, Germantown, MD). RNA was extracted from platelets with the RNeasy Plus Mini Kit (Qiagen), and first strand complementary DNA (cDNA) was prepared using the First Strand cDNA Synthesis Kit (Qiagen). All DNA and messenger RNA (mRNA) samples were quantified using a NanoDrop 2000 spectrophotometer (ThermoFisher Scientific, Waltham, MA) and stored at 4°C (DNA) or —80°C (mRNA) until use.

PCR and nucleotide sequence analysis of *ITGA2B* and *ITGB3* DNA/platelet mRNA

Briefly, polymerase chain reaction (PCR) was accomplished using paired sets of primers designed to amplify all 30 exons and flanking sequences for each exon of *ITGA2B* and all 15 exons and immediate flanking sequences of *ITGB3*, based on published gDNA sequences (supplemental Methods 4).[7,8] The sequences of the primers used for PCR amplification of the exons, adjacent intronic regions, and 5′ and 3′ untranslated regions are shown in supplemental Table 3A-B. PCR was performed using 50 ng of gDNA and 1U Platinum *Taq* DNA polymerase (ThermoFisher Scientific) in 25 μL, containing 20 mM of Tris-HCl (pH 8.4), 50 mM KCl, 2 mM $MgCl_2$, 0.2 mM each deoxynucleotide triphosphate, and 0.2 μM of each primer. The sequences of the primers used for PCR amplification of the *ITGA2B* and *ITGB3* cDNA are shown in supplemental Table 3C-D.

Site-directed mutagenesis of *ITGB3* cDNA and generation of constructs

Human αIIb and β3/pcDNA3 plasmids were kindly provided by Peter Newman (Versiti Blood Research Institute, Milwaukee, WI). Supplemental Table 4 lists each plasmid construct cloned and supplemental Table 5 identifies the mutagenesis primers used to generate these constructs. Site-directed mutagenesis of the β3/pcDNA3 was performed using a QuikChange II Site-Directed Mutagenesis Kit (Qiagen) following the manufacturer's instructions. Nucleotide changes and the fidelity of nontargeted sequences were verified by DNA sequence analysis.

Immunocytometric analysis of mutants expressed on HEK293FT

Plasmids encoding WT αIIb, altered forms of (F,S,W,A,Y)153β3, and enhanced GFP (EGFP) were cotransfected into HEK293FT cells. Twenty-four hours after transfection, cells were incubated with distinct mAbs: AP3 (β3), VIPL2 (β3), 10E5 (αIIb), HIP8 (αIIb), AP2 (αIIbβ3), and 7E3 (αIIbβ3) individually in buffer containing Ca^{2+}/Mg^{2+} or Ca^{2+}/Mn^{2+}. EGFP was used as transfection marker. Cells were washed once after 1°mAb before fluorophore-conjugated 2°Ab incubation. The EGFP-positive cells were analyzed by immunocytometry to measure mAb binding. Data are presented as percentage of MFI of WT for individual mAb binding.

Ligand binding assay of F153β3 mutants

The PAC-1 binding in physiological Ca^{2+}/Mg^{2+} condition or stimulated by Ca^{2+}/Mn^{2+} or overexpression of GFP-tagged talin-head (GFP-TH) domain was performed as described.[30] Fibrinogen (2 mg/mL) was used to inhibit PAC-1 (10 μg/mL) binding in both Ca^{2+}/Mg^{2+} and Ca^{2+}/Mn^{2+} conditions. PAC-1 binding and β3 surface expression (AP3 binding) were quantitated using immunocytometry. β3 and GFP double-positive cells were analyzed for the GFP-TH–induced PAC-1 binding assay. PAC-1 binding was normalized as the MFI in percentage of β3 expression.

Statistical analysis

Data are shown as mean ± standard error of the mean from at least 3 independent experiments unless specified. Parametric unpaired 2-tailed Student *t* test was performed for statistical analyses using GraphPad Prism software (GraphPad Software, La Jolla, CA).

In silico models

Ribbon diagrams of αIIbβ3 structures were generated based on 2vdo or 3fcs PDB file using PyMOL (Schrödinger, LLC, Boston, MA).[31]

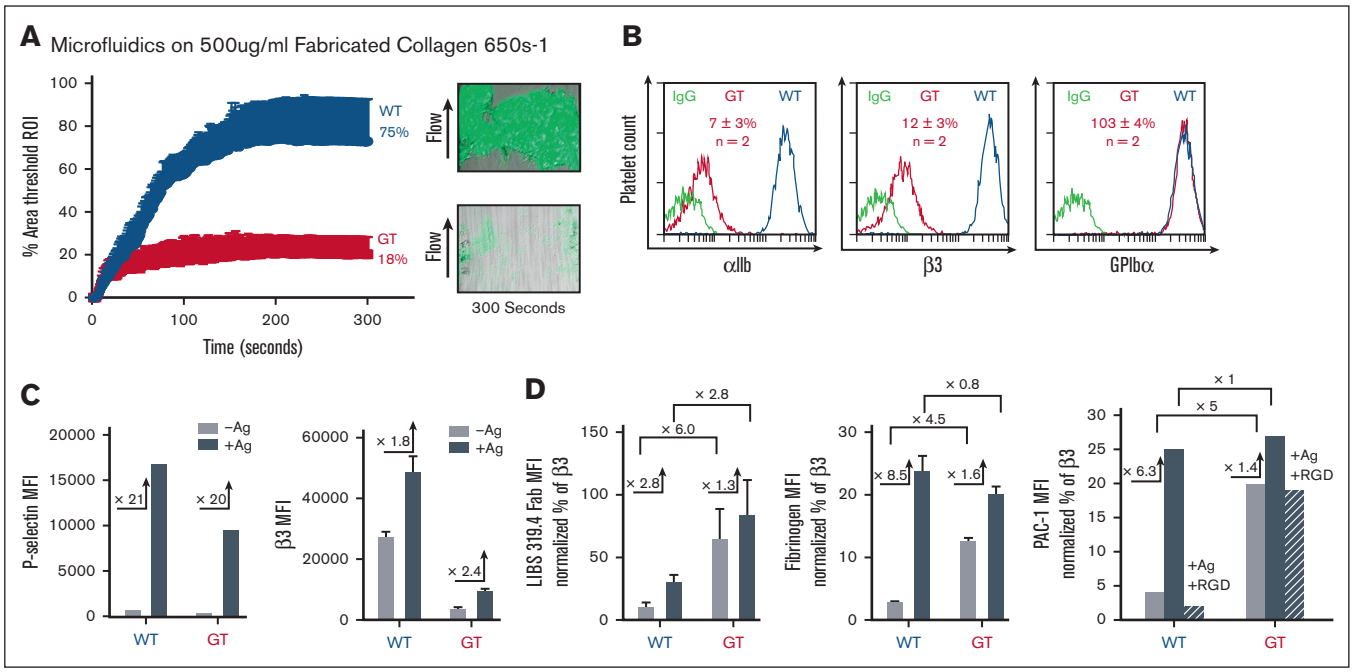

Figure 1. Microfluidic and immunefluorescent cytometric analysis of patient platelets show reduced levels of a constitutively active integrin αIIbβ3 with some ability for platelet adhesion/aggregation consistent with a variant form of GT. (A) Microfluidic chamber analysis of whole blood adhesion/aggregation on collagen under physiological flow conditions. Anticoagulated whole blood from patient and control was 3,3′-dihexyloxacarbocyanine iodide labeled and perfused over fabricated type I collagen (350-500 μg/mL) coated microfluidic devices at 650 s^{-1} for 300 seconds. The percent surface area of platelets adhering and aggregating to the collagen matrix region of interest (ROI) was measured over time (seconds) and quantified at 17.8% ± 0.2% for GT vs 75.1% ± 1.3% for WT (n = 2 in triplicate ± standard error of the mean [SEM]) (left). Representative images taken from paired, representative flows demonstrate significant but visibly decreased surface area and aggregation of GT whole blood compared with WT control (n = 2 in triplicate ± SEM) (right). (B) Immunofluorescent analysis αIIbβ3 expressed on the platelet surface using mAbs specific for human αIIb (CD41, left) and β3 (CD61, middle) observed that platelets from patient with GT (red line) have significantly reduced MFI levels of integrin αIIb (7% ± 3%) and β3 (12% ± 3%) compared with that of WT (blue line), MFI arbitrarily set at 100% (n = 2 ± SEM). As a control for surface expression of a receptor not affected by GT, the MFI for GT GPIbα (103% ± 4%) was nearly equal to WT control with an Ab to human CD42b (n = 2 ± SEM) (right). A nonspecific mAb serves as an isotope negative immunoglobulin G (IgG) control (green line, all). (C) Immunofluorescent cytometric analysis for detection of P-selectin and αIIbβ3 receptor mean fluorescence intensity (MFI) levels on surface of platelets isolated from whole blood from WT control and patient with GT. Platelets were incubated in buffer (−Ag, light grey bar) or treated for 30 minutes with platelet activation agonists (+Ag, dark grey bar). Data are represented in each bar graph as MFI of measurements for the detection of mAbs recognizing increase in surface expression of P-selectin (CD62) as a positive control for platelet activation (n = 2) (left) and β3 (AP3) fold-increase in receptor expression (x) (n = 1 in triplicate + SEM) (right). Analysis with a nonspecific IgG mAb and a CD42 mAb served negative controls for Δ receptor level are not shown (n = 1 in triplicate + SEM). See Methods for further detail. (D) Immunofluorescent cytometric analysis demonstrating ability of WT and GT platelet surface expressed αIIbβ3 to bind "activation-sensitive" reagents listed under quiescent and activating conditions. The bar graph data sets are presented as MFI "activation-sensitive" reagent binding that is normalized to the percentage of β3 receptor density level detected by MFI of a "activation-nonsensitive" reagent AP3 measured on WT and GT platelets, respectively, in section C. Alexa Fluor 647–labeled Fab of mAb 319.4 (recognizing a LIBS exposed on β3) binding in absence of agonist (−Ag, light grey bar) or presence of platelet activation agonists (+Ag, dark grey bar) is shown (left). This is a representative graph using 1 (319.4) of 3 distinct LIBS Abs (n = 3 in triplicate + SEM). The binding of Alexa Flour 488–labeled human fibrinogen under quiescent (−Ag) or activating (+Ag) (n = 2 + SEM) is shown (middle). The binding of mAb fluorescein isothiocyanate–PAC-1 (fibrinogen mimetic Ab) under quiescent (−Ag) or activating (+Ag) (n = 2) is shown (right). Note, inhibition of PAC-1 binding with RGD peptide was measured in the presence of agonist (+Ag +RGD, striped bar, right) (n = 1). Alexa Fluor–labeled goat anti-mouse nonspecific IgG Abs served as negative controls (not shown) (n = 2). Please see Methods for further details.

Results

Patient history

A Hispanic male diagnosed with GT since age 5 drew the attention of this study in his mid-40s because of his mild bleeding history. Remarkably, he has engaged in lifelong strenuous physical activities and contact sports without serious bleeding. He underwent dental procedures without preventive therapy and did not bleed excessively. Of note, platelet transfusion(s), recombinant factor VIIa, and antifibrinolytics were administered during major trauma and surgeries owing to the diagnosis of GT.

Analysis of GT platelet: number, function, and αIIbβ3 receptor

Consistent with the general diagnosis of GT, complete blood count analysis showed the platelet number to be on the low end of normal range (~150 × 10^3 platelets per μL) and within normal range for mean platelet volume 10.3 fL (n = 3) (supplemental Table 1). To confirm GT diagnosis, ex vivo functional analysis with patient PRP showed appreciable aggregation with ristocetin (supplemental Table 2). Although, platelets failed to aggregate in response to ADP, thrombin, and collagen compared with a normal WT control

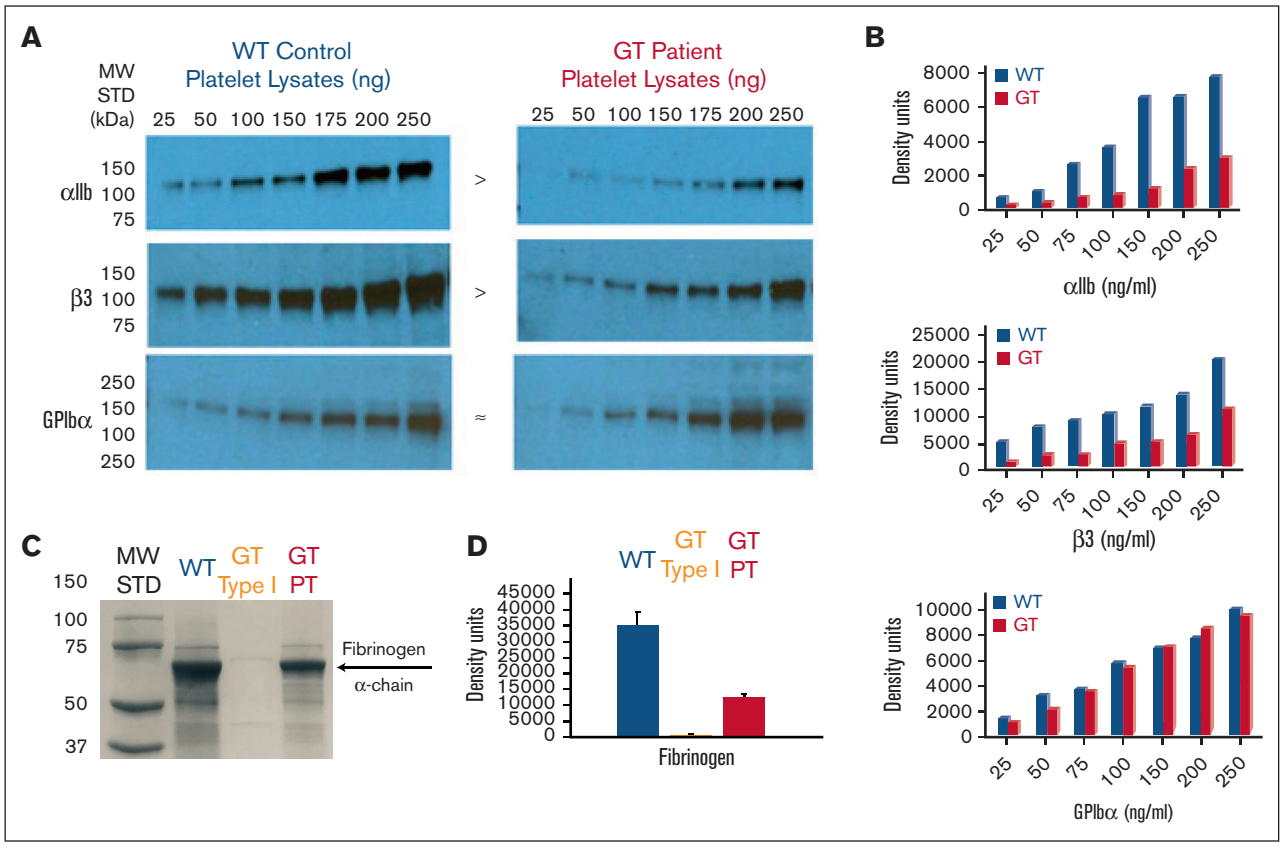

Figure 2. Quantitative analysis of the patient's platelet proteins lysed in SDS show reduced integrin αIIbβ3 and fibrinogen levels consistent with variant form of GT. (A) Immunoblot analysis using Abs specific for detection of αIIb, β3, or GPIbα within platelet protein lysates. Increasing quantities of SDS–platelet protein lysates ranging from 25 to 250 ng were loaded into separate lanes of 10% polyacrylamide gels (PAGEs) and electrophoresed under nonreducing conditions. Following transfer to nitrocellulose, the blots were incubated with goat anti-human polyclonal antibodies to αIIb (136 kDa), β3 (125 kDa), or a mAb to human GPIbα (165 kDa). Immunoreactive bands were detected with an horseradish peroxidase–conjugated 2°Ab followed by chemiluminescence exposure on radiograph film or a digital imager. The result shown is a representative blot ($n \geq 3$ at 7 different lysate concentrations) demonstrating αIIb and β3 appear present at reduced density levels in the GT lysates compared with the WT control, whereas GPIbα appears at similar levels in GT vs WT. (B) Quantitative band density measurements performed with Image J software using photographic film of the immunoblots in panel A exposed to chemiluminescence demonstrate that patient with GT αIIb (30% ± 8%) and β3 (39% ± 11%) is present at reduced levels when comparing the band density with the WT control. As anticipated, the platelet GPIbα levels of patient with GT (94% ± 11%) are nearly identical to a WT control arbitrarily set at 100% in each image. The graphs show MFI in density units for measurements at different concentrations in panel A and converted to percentage ± SEM of WT arbitrarily set at 100% for each representative blot ($n = 4$). (C) Western immunoblot analysis of platelet protein lysates to detect fibrinogen. Protein (10 μg) was loaded onto a 4% to 20% gradient PAGE and SDS-PAGE performed under reducing conditions. Following transfer to nitrocellulose, the blot was incubated with mouse mAb (5C5) directed against the fibrinogen α-chain (60 kDa). Immunoreactive bands were detected by horseradish peroxidase–labeled m-IgGκ binding protein, followed by chemiluminescence and detection on photographic film or digital analyzer. As expected, fibrinogen detected in WT platelets was arbitrarily set as the normal level in the (+) control (blue). The apparent absence of fibrinogen in patients with GT type I (αIIbβ3-deficient) platelets served as a (–) control (yellow). Although in stark contrast, appreciable levels were observed in our sample from patient with GT (red). Shown is results of 1 representative blot ($n = 4$) measured at 3 different exposure times. (D) Fibrinogen band density measurements performed on immunoblot in panel C with Image J software on a scan of the photographic film or digital image used to quantitate the protein level in platelet lysates showed that fibrinogen of patients with GT is present at 34% ± 3% of WT levels of fibrinogen consistent with the levels of αIIb and β3 detected in panel C, while type I GT (–) control had 1.2% ± 0.7% of normal levels. Shown is 1 representative analysis ($n = 4$ + SEM) measure for at least 3 different exposure times. MW, molecular weight; SDS, sodium dodecyl sulfate; STD, standard.

(supplemental Figure 1). Interestingly, whole blood microfluidics analysis performed ex vivo on a collagen-coated surface revealed that the GT platelets could adhere and aggregate using physiological flow conditions (650 s^{-1}) to the collagen surface at moderate levels (17.8% ± 0.2%) of the area threshold compared with a WT control (75.1% ± 1.3%) covering a relatively equal area of interest. This may likely account for the patient's relatively mild bleeding history (Figure 1A). Next, immunocytometry revealed that GT platelets had significantly reduced surface expression of integrin αIIb (7% ± 3%) and β3 (12% ± 3%) compared with a normal WT control arbitrarily set at 100%. As anticipated, GPIbα was detected at nearly equal levels in GT vs WT platelets (103% ± 4%) (Figure 1B). Because the patient only has a mild bleeding history with reduced αIIbβ3 levels, immunocytometry was used next to investigate the relative activation state of αIIbβ3 on quiescent and activated platelets. As anticipated, GT and WT platelets both showed a significant increase (20×) of the α-granule protein (P-selectin) on the platelet surface upon treatment with an agonist (+Ag) of platelet activation (Figure 1C panel 1). In addition, measurement of the MFI for β3 indicated that αIIbβ3 density levels also

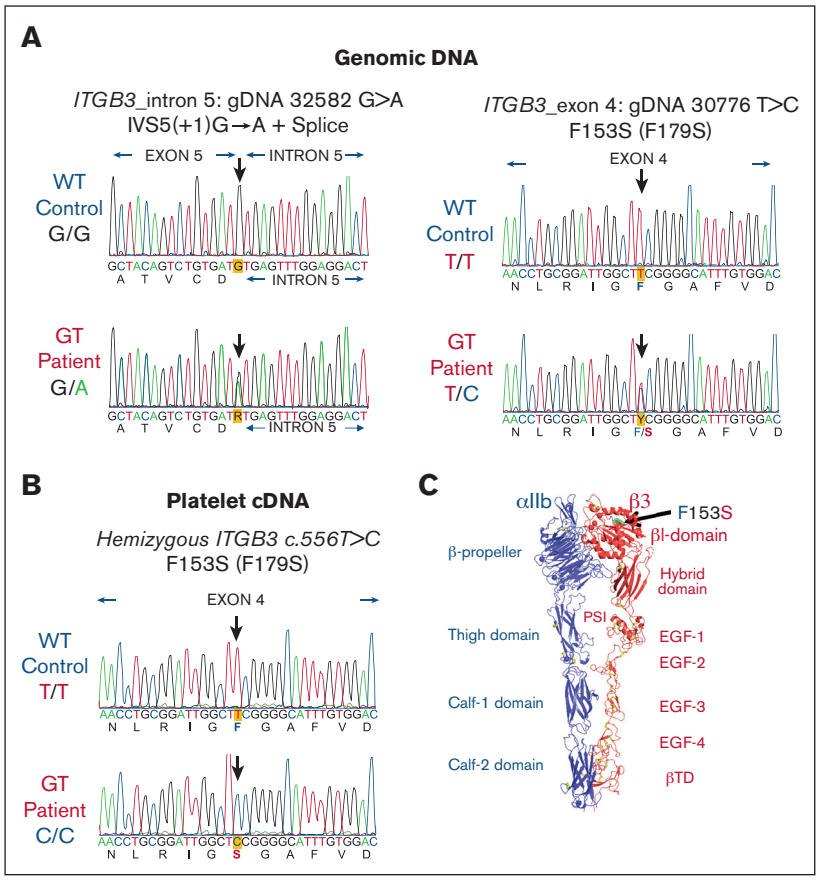

Figure 3. Mutation analysis of *ITGB3* showed that a novel mutation F153S (F179S) in exon 4 and an intronic mutation IVS5(+1) G>A are located on different alleles. (A) Electropherograms of gDNA sequencing reveal a previously reported splice site mutation in intron 5: IVS5(+1) G>A (left) and a novel missense mutation in exon 4 c.556T>C encoding F153S (F179S numbering with cleaved propeptide) (right). The precise nucleotide of each mutation is indicated by a heavy arrow (n = 2 in triplicate with forward and reverse primers). (B) Platelet cDNA sequencing analysis detected only 1 transcript with *ITGB3* mutation: c.556 T>C (F153S or F179S). Sequence analysis primary cDNA (n = 1 in triplicate using forward and reverse primers). The cDNA PCR products were also cloned into a plasmid and sequence analysis confirmed GT hemizygous expression (n = 20 clones using forward and reverse primers). (C) A molecular ribbon diagram designed with PyMol software depicting an extended conformation of αIIbβ3 generated from the crystal structure in the PDB 3fcs shows the location of F153Sβ3 as green sticks and dots.[31] Metal ions are shown as blue spheres. Disulfide bonds are shown as yellow sticks.

increased on WT (1.8×) and GT (2.4×) platelets upon activation (Figure 1C panel 2). GT platelets continued to display a moderate 15% (–Ag) to 20% (+Ag) of normal β3 levels. Thus, P-selectin and β3 levels each increased upon agonist treatment, presumably owing to the change in platelet shape and granular secretion causing additional receptor mobilization to the surface (Figure 1C). However, in stark contrast to WT control, GT quiescent platelets (–Ag) bound activation-dependent Abs (LIBS-319.4 and PAC-1) and fibrinogen at ~5× higher levels than WT quiescent platelets suggesting that GT αIIbβ3 existed in an extended conformation consistent with an intrinsic activation phenotype (Figure 1D). Interestingly, treatment of platelets with an RGD peptide only inhibited PAC-1 binding to GT platelets to preactivation levels, different from complete inhibition of WT platelet's ability to bind PAC-1 (Figure 1D panel 3).

Western immunoblot analysis was performed to quantitate the total αIIbβ3 within platelet protein lysates (Figure 2A). Measurement of the density of each band confirmed that GT platelets had reduced levels of αIIb (30% ± 8%) and β3 (39% ± 11%) compared with that of the WT control (Figure 2B). As anticipated, GPIbα was detected at nearly equal levels in GT vs WT platelets (94% ± 11%) (Figure 2B). This outcome is again consistent with variant type GT classification.[10] Immunoblot analysis was also performed on platelet lysates to measure fibrinogen levels (Figure 2C). Density measurements detected background fibrinogen levels (1.2% ± 0.7%) in the type I GT (–) control, whereas the GT variant had (34% ± 3%) of normal WT fibrinogen levels arbitrarily set at 100% (Figure 2D). Interestingly, the reduced level of fibrinogen in GT variant platelets is proportional to the decreased levels of αIIbβ3 in GT vs WT platelets (comparing panels B and D, Figure 2B,D). Finally, immunofluorescent confocal microscopy with washed and fixed/permeabilized platelets localized fibrinogen in a dispersed granular pattern in the GT and WT samples. Note, consistent with the immunoblot analysis, fibrinogen appeared at reduced fluorescence intensity in GT platelets (supplemental Figure 2). This result indicates that fibrinogen may spontaneously bind to the surface of quiescent GT platelets, which can then undergo αIIbβ3 receptor–mediated endocytosis as observed for the WT control.

ITGB3 sequencing reveals hemizygous expression of a mutant form of a highly conserved residue

All 30 exons of the *ITGA2B* and 15 exons of *ITGB3* with their intronic splicing signals were amplified by PCR and screened by Sanger sequence analysis of gDNA isolated from leukocytes. Two distinct mutations were identified within *ITGB3* (Figure 3A). The first mutation was located on intron 5, 1 nucleotide after the end of exon 5 with a substitution of G>A (lower left panel of Figure 3A). This splice site mutation IVS5(+1)G>A has been previously reported in the MCW GT database (Human Gene Mutation Database ID: CS011047) and is associated with type I GT.[32,33] The second anomaly is a previously unreported mutation detected on exon 4 of *ITGB3* as a single nucleotide T556C substitution

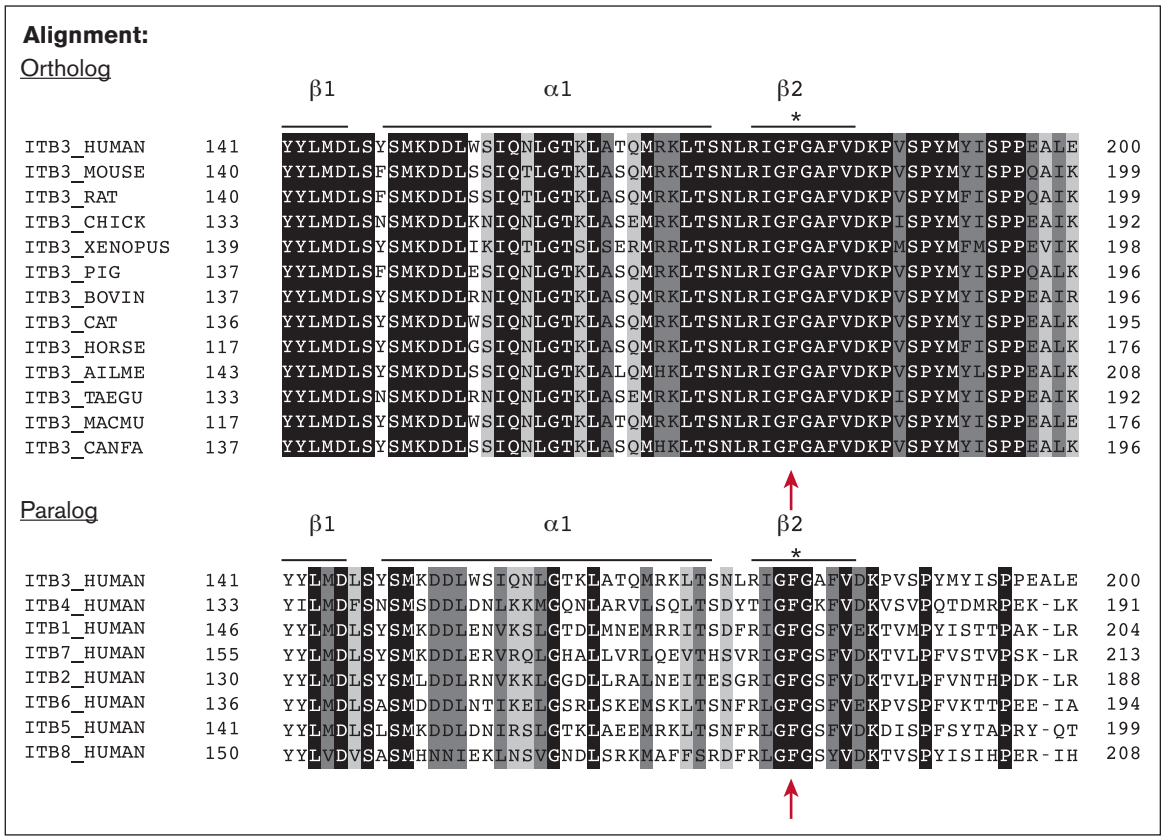

Figure 4. Protein sequence analysis shows amino acid F153 is completely conserved among β-integrin subunits. Sequence alignment of partial amino acid sequence of *ITGB3* (βI-domain, β2-strand) from various species (ortholog alignment) and from various human β-subunits (paralog alignment) indicates that phenylalanine (F)153 mature β3-subunit (amino acid number is 179 including propeptide sequence) is 100% conserved among species and in all human integrin β-subunits.

(lower right panel of Figure 3A). Additional sequence analysis of 20 PCR *ITGB3* introns 3 to 5 gDNA clones verified that each mutation was on a different allele confirming compound heterozygosity (not shown). Remarkably, sequence analysis of platelet cDNA revealed the unique presence of only 1 transcript for the exon 4 *ITGB3* mutation: c.556 T>C encoding a single amino acid change from Phe153 to Ser (F153S) (Figure 3B) suggesting that the intron 5 splice variant was degraded rapidly to create a hemizygous state. Structural analysis shows location of the F153S mutation on the head of the βI-domain of β3 subunit (Figure 3C). Sequence alignment shows conservation of β3 (βI-domain, β2-strand) from various species (ortholog alignment) and among various human β-subunits (paralog alignment) demonstrating that F153 is 100% conserved. This indicates that preservation of this structure likely plays an essential role in integrin function (Figure 4).

F153Sβ3 substitution disrupts integrin expression and function

In silico modeling and mutagenesis studies were performed for αIIb-F153Sβ3 to investigate if substitution from a bulky aromatic to small amino acid residue can affect αIIbβ3 structure/function. The structure superimposition shows that F153 is buried underneath the α2-helix in both active (open) and resting (closed) βI-domain conformation (Figure 5A). A previously unrecognized inward movement of α2-helix was visualized in the active conformation of βI-domain (Figure 5A). A closer view of the β3 structure shows that F153 resides on the β2-strand, with the bulky side chain filled in between α2-helix and β2-strand (Figure 5B). The bulky aromatic structure of F153 appears capable of limiting the inward movement of α2-helix and, thus, helps maintain the resting conformation (Figure 5B, top). The substitution from a bulky aromatic, nonpolar F to a small, polar S appears to allow additional space for α2-helix to assume an active conformation (Figure 5B, bottom). Cell surface expression measured by anti-β3 (mAb AP3) showed a dramatic reduction of αIIb-S153β3 expression (~15% of WT levels) (Figure 5C). This result was further confirmed by the detection of αIIb-S153β3 at reduced levels (~10% to 20% of WT) with a panel of mAbs (*10E5* and *HIP8* that recognize αIIb; *VIPL2* against β3; *AP2* and *7E3* against αIIbβ3 complex) (Figure 5C). This finding is consistent with decreased levels of β3 (~12% to 20% of WT) detected on GT platelets in Figure 1B-C and further supports that the F153Sβ3 mutation adversely affects αIIbβ3 biosynthesis and surface expression. Additional analysis of integrin outside-in activation with Mn^{2+} shows as expected, WT αIIb-F153β3 could only bind PAC-1 in the presence of Mn^{2+} (Figure 5D). In contrast, αIIb-S153β3 bound PAC-1 significantly greater than αIIb-F153β3 in both resting (Mg^{2+}) and active (Mn^{2+}) conditions (Figure 5D). PAC-1 binding was inhibited by the presence of fibrinogen. These data are consistent with the GT platelet assays showing a constitutively active conformation of αIIbβ3 owing to the F153Sβ3 mutation.

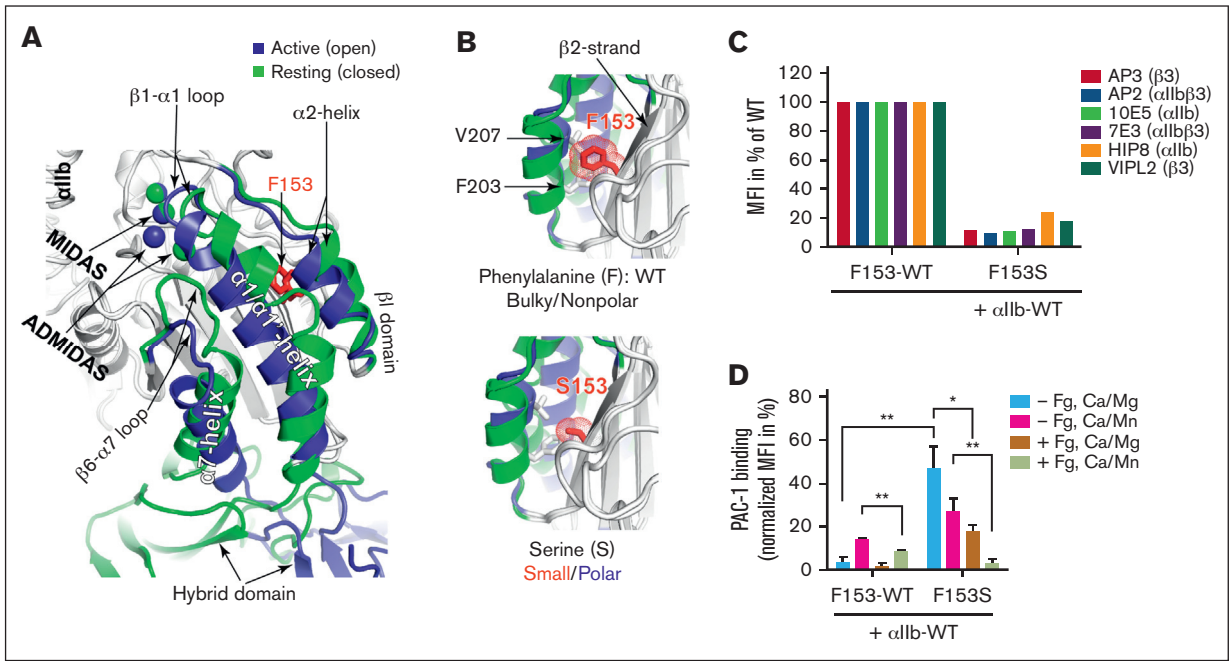

Figure 5. The F153Sβ3 mutation exerts functional effect on αIIbβ3 surface expression and ligand binding. (A) Superimposition of crystal structures of normal αIIbF153β3 globular head region, highlighting the structural changes of β3 I domain from resting (in green) to active state (in blue). The metal ions of MIDAS and ADMIDAS are shown as spheres. The red side chain localizes 153aa in the core of βI-domain in the central part of β-sheet number 2, which is underneath the α2-helix. An inward movement of α2-helix is noted along with the inward movement of β1-α1 loop and α1/α1′-helix, and the downward movement of β6-α7 loop and α7-helix. The structural comparison was made using PDB 2vdo and 3fcs with PyMol. (B) In silico mutagenesis of F153β3. The hydrophobic interaction between F153 and the residues V207 and F203 of α2-helix in the WT form is shown (top). The S153 mutation losses the bulky hydrophobic contact with the α2-helix is shown (bottom). The F153S mutation may render αIIbβ3 constitutively active by facilitating an unrestricted inward movement of α2- and α1-helices during the conformational transition of the β3 integrin from a resting to an active state, because bulky/nonpolar to small/polar amino acid side chain provide space for structural change to facilitate increased movement. Enlarged images of the β2-strand βI-domain also predict the effect on Van der Waal force (red cloud) resulting from the change in structure of the β3 153aa side-chain going from bulky F to small S. Changes induced by F153Sβ3 are depicted in the smaller and hydrophilic serine residue, which also may introduce disorganization by permitting entrance of water molecules that may competitively form H-bonds with oxygen atoms or NH_2-groups of constituent amino acid of the core and disrupt structure. In silico mutagenesis were made in PyMol using PDB 2vdo and 3fcs. (C) Immunofluorescent cytometric analysis detection of level of cell surface expression of αIIbβ3 using distinct mAbs: 10E5 and HIP8 specific for αIIb, AP3 and VIPL2 recognizing β3, and AP2 and 7E3 against the αIIbβ3 complex. Integrin αIIb and F153β3 or S153β3 subunits plus GFP were cotransfected into HEK293FT cells. Harvested cells were incubated with indicated mAb and then GFP^+ cells were analyzed for MFI of mAb binding on the cell surface via immunocytometry. The S153β3 mutant is observed to be expressed at ~10% to 20% of F153β3 (WT). Data are presented as percent of WT control, MFI arbitrarily set at 100% (n = 3). (D) Measurement of αIIb-F153Sβ3 ability to bind activation-dependent mAb "PAC-1" in the absence (–Fg) or presence (+Fg) of unlabeled fibrinogen. αIIb and F153β3 or S153β3 subunits were cotransfected into HEK293FT cells and harvested cells then incubated with or without unlabeled fibrinogen in the presence of Ca^{2+}/Mg^{2+} (Ca/Mg) or an extracellular αIIbβ3 agonist Ca^{2+}/Mn^{2+} (Ca/Mn) before the addition of PAC-1. Integrin-positive cells were analyzed for PAC-1 MFI binding. The bar graph demonstrates PAC-1 binding that was normalized to the total MFI in percent of each form of F153β3 or S153β3 expression in panel C . Data are presented as MFI in percentage + SEM (n ≥ 3) and unpaired 2-tailed Student *t* test was performed to compare the mutants with WT under the same condition or as indicated. $*P < .05$, $**P < .01$.

Additional mutagenesis studies demonstrate a vital structural role for a bulky aromatic, nonpolar 153aa of β3 in regulating αIIbβ3 activation

The WT and 4 alternative forms of 153aa on β3 were generated to further characterize how change in the size and charge of the side-chain may affect integrin activation. The aromatic structure of W and Y were used to compare with F, whereas the small, nonpolar A was used to compare with small, polar S (Figure 6A). The activation status of each αIIbβ3 construct was assessed by coexpression with either a GFP control or GFP-TH to induce integrin inside-out activation. Cell surface expression measured by anti-β3 mAb AP3 showed a dramatic reduction of αIIb-S153β3 expression, whereas expression levels of αIIb-(A,Y,W)153β3 mutants were not significantly different from the WT αIIb-F153β3 (Figure 6B). Interestingly, PAC-1 binding showed a remarkable correlation between residue size at position 153 and the activation status of αIIbβ3 (Figure 6C). Specifically, αIIb-(S,A)153β3 were both in a constitutively active conformation capable of binding PAC-1 in the absence/presence of inside-out activation with GFP-TH (Figure 6C). Of note, the W153β3 mutant activation was indistinguishable from WT F153β3, whereas Y153β3 mutant suppressed GFP-TH–induced αIIbβ3 activation, suggesting that addition of a polar charge on a bulky aromatic amino acid may hinder the change of α2-helix toward an active conformation (Figure 6C). These data demonstrate that a bulky aromatic, nonpolar residue on 153 of β3 appears essential for maintaining normal integrin function because a small amino acid substitution (nonpolar or polar) at this position (as observed in the patient with GT) renders αIIbβ3 constitutively active on the platelet surface.

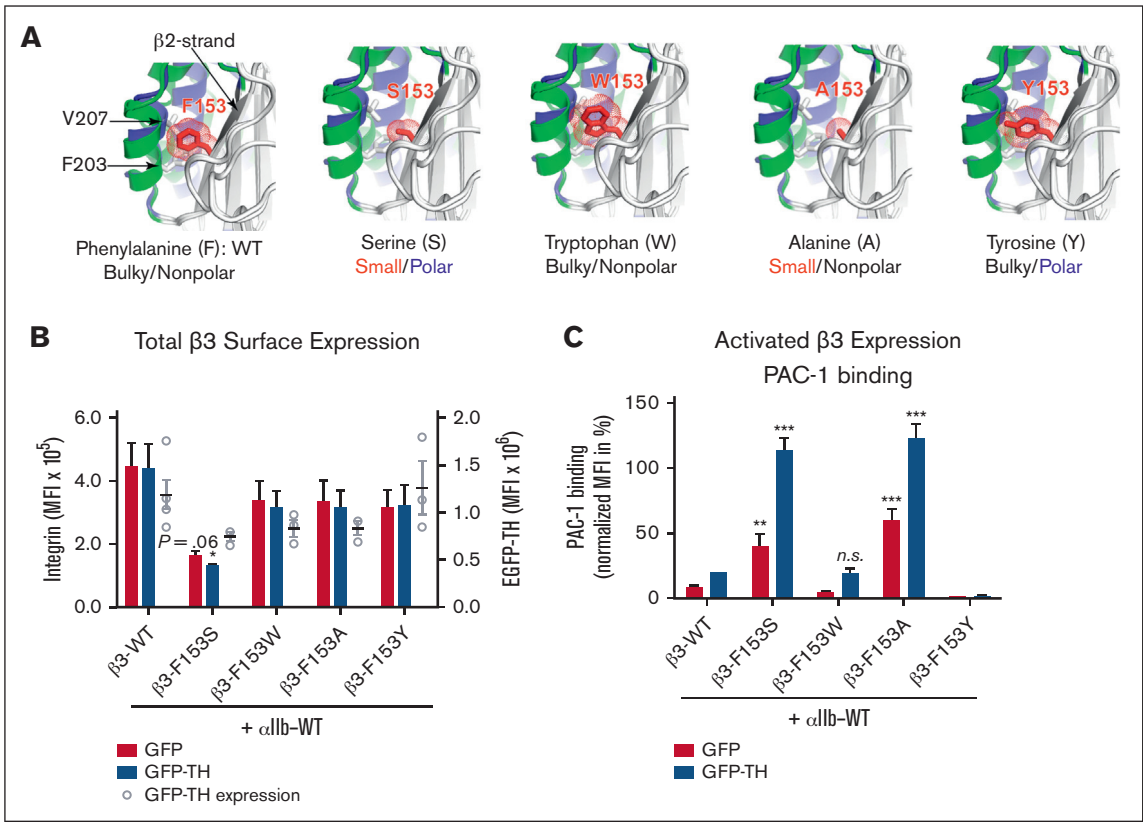

Figure 6. Expression analysis of several mutants suggests that 153aa of β3 with a bulky aromatic and nonpolar structure can maintain normal integrin expression and function. (A) In silico mutagenesis of F153β3 with small and bulky amino acid shows the space filling effect of the sidechain volumes. The F153S and F153A mutations may render αIIbβ3 constitutively active by facilitating an unrestricted inward movement of α2-helix during the conformational transition of the β3 integrin from a resting to an active state, whereas the F153W and F153Y may limit such movement. In silico mutagenesis were made in PyMol using PDB 2vdo and 3fcs. The resting and active conformations of α2-helix are highlighted in green and blue, respectively. (B) Immunofluorescent cytometric analysis to quantitate MFI expression levels of transgenic mutant β3-integrin on the surface of HEK293FT. Integrin αIIb and mutated β3 subunits plus GFP or GFP-TH (talin-head integrin activation construct) were cotransfected into HEK293FT cells. Harvested cells were then labeled with an anti-β3 mAb (AP3). GFP immunofluorescence was used as a control for transfection efficiency and integrin double-positive cells were analyzed for their MFI of either AP3 or GFP by immunocytometry. Results show that there is a significant reduction in the cell surface integrin expression of GT mutation (β3-F153S) compared with the WT control (β3-WT) whereas there is no statistical significance in total β3 surface expression between the WT and the other β3 variants (F153W, F153A, and F153Y). Data are presented as mean MFI + SEM (n ≥ 3) and unpaired 2-tailed Student *t* test was performed to compare the mutants with WT under the same condition or as indicated ($P = .06$). (C) Maximum integrin activity after stimulation with GFP-TH is detected by the binding of PAC-1, which is specific for the active conformation of αIIbβ3. Integrin αIIb and indicated β3 subunits plus GFP or GFP-TH are cotransfected into HEK293FT cells. Integrin and GFP double-positive cells were analyzed for the PAC-1 binding via immunocytometry. PAC-1 binding was quantified and normalized to the total integrin expression showing that (1) bulky aromatic, nonpolar (F,W) are activated identically; (2) bulky aromatic polar (Y) activation is negatively disrupted; and (3) small, polar and nonpolar side-chains (S,A) place αIIbβ3 in a constitutively activate confirmation without (red bar) or with (blue bar) talin head domain present. PAC-1 binding is normalized to the total integrin expression. Data are presented as MFI in percentage + SEM (n ≥ 3) and unpaired 2-tailed Student *t* test was performed to compare the mutants with WT under the same condition or as indicated. *$P < .05$, **$P < .01$, ***$P < .001$. n.s., not significant.

Discussion

This study characterizes a novel variant GT associated with a gain-of-function F153Sβ3 mutation within the βI-domain of αIIbβ3. The GT platelets contain a heterozygous *ITGB3* variant of F153S and a loss-of-expression mutation, suggesting that the novel phenotype is solely attributed to the F153S mutation. Interestingly, a paradox was presented because the patient was clinically diagnosed with GT based upon blood tests, although he does not display the GT bleeding phenotype because his platelets have functionality in vivo (evidenced by >40 years of mild bleeding without severe hemorrhage amid a reportedly very physically active lifestyle prone to injury). This observation inspired a detailed examination to unravel the enigma presented because the patient's platelets failed to aggregate ex vivo in response to all physiologic agonists except ristocetin consistent with the clinical diagnosis of GT.[13] Furthermore, there was significantly decreased expression of αIIbβ3 on the surface of the patient's platelets, although the GT platelets appear to maintain relatively normal function including fibrinogen storage and α-granule secretion. Interestingly, a microfluidic assay using whole blood demonstrated that the platelets retain a modest level of adhesion and aggregation on a collagen-coated chamber under physiological shear flow. This result is consistent with the observation of viable hemostatic function in vivo. Remarkably, these GT platelets bind fibrinogen and activation-dependent Abs in the

absence or presence of physiological agonists of platelet activation demonstrating that αIIbβ3 exists in a constitutively active conformation. Different from other previously described GT variants with gain-of-function β3 mutations (including the I-EGF domain mutations and a recent βI N331S mutation),[34] this patient with F153Sβ3 GT exhibits no apparent macrothrombocytopenia with a mild bleeding phenotype, suggesting discovery of a unique GT variant.

Structural and functional analysis indicate a plausible molecular mechanism for rendering F153Sβ3 in a constitutively active conformation. Crystallographic and mutagenesis studies depict major structural changes occurring within the α1- and α7-helices and their connecting loops upon βI-domain activation.[23,35] This report observed a subtle conformational change of α2-helix in the active state of βI-domain, the significance of which in regulating integrin activation was not appreciated previously. Furthermore, mutagenesis studies suggest that the bulky aromatic, nonpolar sidechain of F153β3 appears to be vital for keeping α2-helix in a normal resting conformation. The hydrophobic interaction between F153 on β2-strand and the conserved F203 and V207 on α2-helix appears essential to limit movement of the α2-helix toward an active state on quiescent platelets, because reducing the size of F153 with the S or A substitution permits increased movement of α2-helix and shifts βI-domain to the active conformation. However, addition of a hydroxy group with a F153Y substitution hinders movement of the α2-helix because αIIbβ3 activation was completely blocked. Thus, the constitutively active F153Sβ3 GT variant reveals new information concerning the regulation of β3 activation through the interaction of a bulky aromatic residue on β2-strand and α2-helix. Further mutagenesis studies examining variants of F203β3 and V207β3 or equivalent F153 mutations in other β-integrins will likely advance our understanding of the mechanism of integrin activation.[36]

Characterization of molecular genetic defects discovered within patients with GT has revealed a wealth of information for >30 years concerning the effect of αIIbβ3 structure on integrin and platelet function.[10,13,14] Many times it has been the rare variant forms of GT including "gain-of-function" mutations of αIIbβ3 that have been particularly interesting because they present a variety of effects on integrin structure/function associated with disease.[10] In this manner, this study reveals a novel GT variant of F153Sβ3 with reduced surface expression but constitutively active phenotype. This finding helps provide new insight on a mutation expressed at subnormal levels but compensated by constitutive activation leading to altered albeit viable platelet function and achieves hemostasis sufficient to permit a mild bleeding phenotype associated with strenuous physical activity, a finding that may reveal a new target on αIIbβ3 for antithrombotic therapy. However, new questions arise that require further study concerning how the F153Sβ3 mutation may alter the kinetics of αIIbβ3 conformational change in resting and activated platelets. This may be clarified with additional analysis of mutant αIIbβ3 response to other physiological ligands or ligand-mimetic inhibitors,[22] such as seen with the RGD peptide. Interestingly, F153β3 permits fibrinogen binding and receptor-mediated endocytosis, although detailed immunogenic studies using confocal and electronic microscopy employing specific markers for fibrinogen and endocytic vesicles may enhance our understanding of the process. Also, it may be of particular interest to hematologists whether the constitutively active phenotype of F153Sβ3 can increase the risk of thrombosis and whether patients with GT with gain-of-function mutations require recombinant factor VIIa as a preventive measure against surgical bleeding. Finally, it is apparent that this patient's mild bleeding phenotype is consistent with intact clot retraction capability. However, measurement of the ability of F153β3 platelets to maintain sustained aggregation, clot retraction, and thrombus formation could provide profound clinical benefit.[37] Technologies generating genetically-altered platelets and megakaryocytes derived from hematopoietic stem cells should aid future efforts to answer these questions.[19,38-40]

Acknowledgments

The authors acknowledge the Children's Research Institute Imaging Core (Milwaukee, WI) for use of its confocal microscope facility and thank Suresh Kumar for the technical support in data acquisition and analysis paid for by a generous gift from the Children's Hospital Foundation (D.A.W.). The authors thank Kristi Norton, B.S., Certified Clinical Research Professional for her tremendous effort serving as the research services program manager at the Hemophilia and Thrombosis Center, Anschutz Medical Campus, University of Colorado (Aurora, CO).

This work was supported partially by grants/support from the National Heart, Lung, and Blood Institute, National Institutes of Health (grants HL131836, HL139825, and HL144457) (J.Z., J.D.P., and C.J.N., respectively); the Health Resources & Services Administration–Maternal & Child Health (5 H30 MC00008-20-00) (C.J.N.); Children's Wisconsin Foundation–Children's Research Institute (CRI21303) (D.A.W.); Midwest Athletes Against Childhood Cancer and Bleeding Disorders Fund (D.A.W.); and generous gifts from John B. and Judith A. Gardetto (D.A.W.), Glanzmann Research Foundation (D.A.W.), and James Swain/ING/Voya (D.A.W.).

The content is solely the responsibility of the author and does not necessarily represent the official views of the National Institutes of Health. Sponsors and funders had no role in study design, data collection and analysis, decision to publish, or preparation of manuscript.

Authorship

Contribution: S.B.K., J.D.P., J.Z., and D.A.W. designed research; S.B.K., A.M.M.T., K.J.A., J.F., H.S.S., L.M.D., H.T.T.N., X.P., C.J.N., and J.Z. performed research and collected data; X.P. and J.Z. contributed new analytic tools; S.B.K., A.M.M.T., K.J.A., J.F., H.S.S., H.T.T.N., X.P., A.T.N., C.J.N., J.D.P., J.Z., and D.A.W. analyzed and interpreted data; S.B.K. and A.M.M.T. performed statistical analysis; and S.B.K., A.M.M.T., K.J.A., A.T.N., J.D.P., J.Z., and D.A.W. wrote the manuscript.

Conflict-of-interest disclosure: D.A.W. is the president of Platelet Targeted Therapeutics, LLC and has equity interest and intellectual property rights in the company. The remaining authors declare no competing financial interests.

X.P. died on 7 July 2021.

ORCID profiles: S.B.K., 0000-0002-5931-5491; K.J.A., 0000-0001-7862-6503; A.T.N., 0000-0002-7878-8307.

Correspondence: David A. Wilcox, Department of Pediatrics, MFRC #6014, Medical College of Wisconsin, 8701 Watertown Plank Rd, Milwaukee, WI 53226; email: dwilcox@mcw.edu; and Jieqing Zhu, Versiti Blood Research Institute, 8727 Watertown Plank Rd, Milwaukee, WI 53226; email: jieqing.zhu@versiti.org.

References

1. Patel D, Vaananen H, Jirouskova M, Hoffmann T, Bodian C, Coller BS. Dynamics of GPIIb/IIIa-mediated platelet-platelet interactions in platelet adhesion/thrombus formation on collagen in vitro as revealed by videomicroscopy. *Blood*. 2003;101(3):929-936.
2. Ma YQ, Qin J, Plow EF. Platelet integrin alpha(IIb)beta(3): activation mechanisms. *J Thromb Haemost*. 2007;5(7):1345-1352.
3. Coller BS, Shattil SJ. The GPIIb/IIIa (integrin alphaIIbbeta3) odyssey: a technology-driven saga of a receptor with twists, turns, and even a bend. *Blood*. 2008;112(8):3011-3025.
4. Durrant TN, van den Bosch MT, Hers I. Integrin alpha(IIb)beta(3) outside-in signaling. *Blood*. 2017;130(14):1607-1619.
5. Wagner CL, Mascelli MA, Neblock DS, Weisman HF, Coller BS, Jordan RE. Analysis of GPIIb/IIIa receptor number by quantification of 7E3 binding to human platelets. *Blood*. 1996;88(3):907-914.
6. Fiore M, Nurden AT, Nurden P, Seligsohn U. Clinical utility gene card for: Glanzmann thrombasthenia. *Eur J Hum Genet*. 2012;20(10):1101.
7. Heidenreich R, Eisman R, Surrey S, et al. Organization of the gene for platelet glycoprotein IIb. *Biochemistry*. 1990;29(5):1232-1244.
8. Zimrin AB, Gidwitz S, Lord S, et al. The genomic organization of platelet glycoprotein IIIa. *J Biol Chem*. 1990;265(15):8590-8595.
9. Bray PF, Barsh G, Rosa JP, Luo XY, Magenis E, Shuman MA. Physical linkage of the genes for platelet membrane glycoproteins IIb and IIIa. *Proc Natl Acad Sci U S A*. 1988;85(22):8683-8687.
10. Nurden AT, Pillois X. ITGA2B and ITGB3 gene mutations associated with Glanzmann thrombasthenia. *Platelets*. 2018;29(1):98-101.
11. Glanzmann E. Hereditare hamorrhagische thrombasthenie: ein beitrag zur pathologie dr blut plattchen [Hereditary hemorrhagic thrombasthenia: a contribution on the pathology of blood platelets]. *J Kinderkr*. 1918;88:113-141.
12. Nurden AT, Pillois X, Fiore M, et al. Expanding the mutation spectrum affecting alphaIIbbeta3 integrin in Glanzmann thrombasthenia: screening of the ITGA2B and ITGB3 genes in a large international cohort. *Hum Mutat*. 2015;36(5):548-561.
13. Botero JP, Lee K, Branchford BR, et al. Glanzmann thrombasthenia: genetic basis and clinical correlates. *Haematologica*. 2020;105(4):888-894.
14. Nurden A. Profiling the genetic and molecular characteristics of glanzmann thrombasthenia: can it guide current and future therapies? *J Blood Med*. 2021;12:581-599.
15. Nurden AT, Fiore M, Nurden P, Pillois X. Glanzmann thrombasthenia: a review of ITGA2B and ITGB3 defects with emphasis on variants, phenotypic variability, and mouse models. *Blood*. 2011;118(23):5996-6005.
16. Ross JE, Zhang BM, Lee K, et al. Specifications of the variant curation guidelines for ITGA2B/ITGB3: ClinGen Platelet Disorder Variant Curation Panel. *Blood Adv*. 2021;5(2):414-431.
17. Buitrago L, Rendon A, Liang Y, et al. αIIbβ3 variants defined by next-generation sequencing: predicting variants likely to cause Glanzmann thrombasthenia. *Proc Natl Acad Sci U S A*. 2015;112(15):E1898-1907.
18. Coller BS. αIIbβ3: structure and function. *J Thromb Haemost*. 2015;13(suppl 1):S17-25.
19. Fang J, Hodivala-Dilke K, Johnson BD, et al. Therapeutic expression of the platelet-specific integrin, alphaIIbbeta3, in a murine model for Glanzmann thrombasthenia. *Blood*. 2005;106(8):2671-2679.
20. Lehmann M, Ashworth K, Manco-Johnson M, Di Paola J, Neeves KB, Ng CJ. Evaluation of a microfluidic flow assay to screen for von Willebrand disease and low von Willebrand factor levels. *J Thromb Haemost*. 2018;16(1):104-115.
21. Schaffner-Reckinger E, Gouon V, Melchior C, Plancon S, Kieffer N. Distinct involvement of beta3 integrin cytoplasmic domain tyrosine residues 747 and 759 in integrin-mediated cytoskeletal assembly and phosphotyrosine signaling. *J Biol Chem*. 1998;273(20):12623-12632.
22. Lin FY, Li J, Xie Y, et al. A general chemical principle for creating closure-stabilizing integrin inhibitors. *Cell*. 2022;185(19):3533-3550.e27.
23. Zhang C, Liu J, Jiang X, et al. Modulation of integrin activation and signaling by alpha1/alpha1'-helix unbending at the junction. *J Cell Sci*. 2013;126(Pt 24):5735-5747.
24. Fang J, Nurden P, North P, et al. C560Rβ3 caused platelet integrin αII b β3 to bind fibrinogen continuously, but resulted in a severe bleeding syndrome and increased murine mortality. *J Thromb Haemost*. 2013;11(6):1163-1171.
25. Wang R, McFarland JG, Kekomaki R, Newman PJ. Amino acid 489 is encoded by a mutational "hot spot" on the beta 3 integrin chain: the CA/TU human platelet alloantigen system. *Blood*. 1993;82(11):3386-3391.
26. Smith PK, Krohn RI, Hermanson GT, et al. Measurement of protein using bicinchoninic acid. *Anal Biochem*. 1985;150(1):76-85.
27. Laemmli UK. Cleavage of structural proteins during the assembly of the head of bacteriophage T4. *Nature*. 1970;227(5259):680-685.
28. Towbin H, Staehelin T, Gordon J. Electrophoretic transfer of proteins from polyacrylamide gels to nitrocellulose sheets: procedure and some applications. *Proc Natl Acad Sci U S A*. 1979;76(9):4350-4354.
29. Du LM, Nurden P, Nurden AT, et al. Platelet-targeted gene therapy with human factor VIII establishes haemostasis in dogs with haemophilia A. *Nat Commun*. 2013;4:2773.
30. Wang Z, Zhu J. Measurement of integrin activation and conformational changes on the cell surface by soluble ligand and antibody binding assays. *Methods Mol Biol*. 2021;2217:3-15.

31. Zhu J, Luo BH, Xiao T, Zhang C, Nishida N, Springer TA. Structure of a complete integrin ectodomain in a physiologic resting state and activation and deactivation by applied forces. *Mol Cell*. 2008;32(6):849-861.

32. French DL, Coller BS. Hematologically important mutations: Glanzmann thrombasthenia. *Blood Cells Mol Dis*. 1997;23(1):39-51.

33. Stenson PD, Mort M, Ball EV, et al. The Human Gene Mutation Database: towards a comprehensive repository of inherited mutation data for medical research, genetic diagnosis and next-generation sequencing studies. *Hum Genet*. 2017;136(6):665-677.

34. Bury L, Zetterberg E, Leinoe EB, et al. A novel variant Glanzmann thrombasthenia due to co-inheritance of a loss- and a gain-of-function mutation of ITGB3: evidence of a dominant effect of gain-of-function mutations. *Haematologica*. 2018;103(6):e259-e263.

35. Xiao T, Takagi J, Coller BS, Wang JH, Springer TA. Structural basis for allostery in integrins and binding to fibrinogen-mimetic therapeutics. *Nature*. 2004;432(7013):59-67.

36. Hynes RO. Integrins: versatility, modulation, and signaling in cell adhesion. *Cell*. 1992;69(1):11-25.

37. Nurden AT. Molecular basis of clot retraction and its role in wound healing. *Thromb Res*. 2022 Aug 19:S0049-3848(22)00350-4. https://doi.org/10.1016/j.thromres.2022.08.010. Epub ahead of print.

38. Wilcox DA, Olsen JC, Ishizawa L, et al. Megakaryocyte-targeted synthesis of the integrin b3-subunit results in the phenotypic correction of Glanzmann thrombasthenia. *Blood*. 2000;95(12):3645-3651.

39. Fang J, Jensen ES, Boudreaux MK, et al. Platelet gene therapy improves hemostatic function for integrin alphaIIbbeta3-deficient dogs. *Proc Natl Acad Sci U S A*. 2011;108(23):9583-9588.

40. Sullivan SK, Mills JA, Koukouritaki SB, et al. High-level transgene expression in induced pluripotent stem cell-derived megakaryocytes: correction of Glanzmann thrombasthenia. *Blood*. 2014;123(5):753-757.